HHS Public Access

Author manuscript

Bioorg Med Chem. Author manuscript; available in PMC 2018 September 25.

Published in final edited form as:

Bioorg Med Chem. 2018 September 15; 26(17): 4787–4796. doi:10.1016/j.bmc.2018.07.034.

An antimycobacterial pleuromutilin analogue effective against dormant bacilli

Maddie R. Lemieux[a], **Shajila Siricilla**[a], **Katsuhiko Mitachi**[a], **Shakiba Eslamimehr**[a], **Yuehong Wang**[b], **Dong Yang**[c], **Jeffrey D. Pressly**[a], **Ying Kong**[c], **Frank Park**[a], **Scott G. Franzblau**[b], and **Michio Kurosu**[a,*]

[a]Department of Pharmaceutical Sciences, College of Pharmacy, University of Tennessee Health Science Center, 881 Madison Avenue, Memphis, TN 38163-0001, United States

[b]Institute for Tuberculosis Research, College of Pharmacy, University of Illinois at Chicago, 833 S. Wood Street, Chicago, IL 60612, United States

[c]Department of Microbiology, Immunology & Biochemistry, University of Tennessee Health Science Center, 858 Madison Avenue, Memphis, TN 38163-0001, United Sates

Abstract

Pleuromutilin is a promising pharmacophore to design new antibacterial agents for Gram-positive bacteria. However, there are limited studies on the development of pleuromutilin analogues that inhibit growth of *Mycobacterium tuberculosis* (Mtb). In screening of our library of pleuromutilin derivatives, UT-800 (**1**) was identified to kill replicating- and non-replicating Mtb with the MIC values of 0.83 and 1.20 μg/mL, respectively. UT-800 also kills intracellular Mtb faster than rifampicin at 2xMIC concentrations. Pharmacokinetic studies indicate that **1** has an oral bioavailability with an average *F*-value of 27.6%. Pleuromutilin may have the potential to be developed into an orally administered anti-TB drug.

Keywords

Pleuromutilin; Antimycobacterial activity; Dormant tuberculosis; Intracellular *Mycobacterium tuberculosis*; Pharmacokinetics

1. Introduction

Mycobacterium tuberculosis (Mtb) can persist in host tissues for months to decades without replicating, yet with the ability to resume growth.[1,2] The ability of Mtb to survive in host macrophages or granulomas by entering the dormant state is one factor that requires the long duration of tuberculosis (TB) chemotherapy.[3] The dormant form of Mtb shows resistance to most of the clinically utilized TB drugs at approved therapeutic concentrations.[4] Over the last 40 years, bedaquiline and delamanid are the only TB drugs that have successfully been

*Corresponding author. Tel.: +1-901-448-1045; fax: +1-901-448-7530; mkurosu@uthsc.edu.

A. Supplementary material

Some assay data, copies of NMR spectra, HPLC chromatogram of new compounds, and assay procedures. This material is available free of charge via the Internet at https://doi.org.

developed into clinical application. However, their usage is restricted to patients who have failed the standard TB regimens. Currently, only a few new drugs have been evaluated in clinical trials.[5,6]

Since the discovery of pleuromutilin from *Basidomycete spp*. in 1952, two drugs (tiamulin and valnemulin) and one drug (retapamulin) were successfully developed as therapeutic agents for veterinary and human applications, respectively. Retapamulin is the first antibacterial agent of the pleuromutilin class for human application; it was approved in 2007 by the FDA for the topical treatment of impetigo and secondary infected traumatic lesions of skin infections caused by Gram-positive bacteria such as *S. aureus*and *S. pyogenes*.[7,8,9] Recently, significant advances were made in the development of pleuromutilin to become a systemic or orally bioavailable antibiotic for MRSA infections (*e.g.* BC-3781 (Nabriva Therapeutics)).[10,11,12] The majority of pleuromutilin derivatives reported to date displays a spectrum of activity focused against Gram-positive bacteria,[13,14,15,16,17,18,19,20,21] and very few analogues have been demonstrated to exhibit antimycobacterial activity. Long et. al. reported moderate activity of valnemulin against *Mycobacterium smegmatis* (MIC 8-16 μg/mL).[22] Tiamulin-like derivatives displayed moderate activity against Mtb (Lotesta et. al., 2011).[23] Dong et. al. reported that C14-*N*-benzylamine substituted pleuromutilin analogues have anti-Mtb activity (60-100% inhibition at 20 μM).[24] Several other pleuromutilin analogues with modifications at C14, C12, C2, C4, C6 and/or C7 were filed in the patents that were evaluated against Mtb (Figure 1).[25,26,27,28,29] In our discovery program for identifying new antimycobacterial pleuromutilin derivatives effective against non-replicating (dormant) form of Mtb, we discovered that an analogue UT-800 (**1**) exhibited strong bactericidal activity against Mtb with the MIC value of 0.83 μg/mL against replicating-Mtb and 1.20 μg/mL against non-replicating-Mtb. Here, we wish to report *in vitro* assay data for **1**, and pharmacokinetic profile and oral bioavailability of **1**.

2. Results and discussion

2.1. Discovery of antimycobacterial pleuromutilin analogues that kill non-replicating Mtb.

We have generated a library of pleuromutilin derivatives aiming at discovering anti-Gram-negative bacterial agents.[30] The same library molecules were evaluated against Mtb ($H_{37}Rv$) in microplate alamar blue assay (MABA). We identified four pleuromutilin analogues which exhibited the MIC_{100} value <6.25 μg/mL against Mtb under aerobic conditions (Figure 2). Interestingly, the identified antimycobacterial analogues are D-leucine derivatives whose core structures are varied by the oxidation states at the C3-carbonyl and C12-vinyl groups.

2.2. Synthesis of antimycobacterial pleuromutilin analogues 1-4.

In order to confirm antimycobacterial activity of four hit compounds and to evaluate their activity against non-replicating Mtb, **1**-**4** were resynthesized according to the procedures established in our laboratory (Scheme 1).[30] The C3-carbonyl group of pleuromutilin (**5**) was reduced with $NaBH_4$ to form the secondary alcohol with *R*-configuration exclusively. The primary alcohol of the C14-side chain was tosylated with TsCl in the presence of *N,N*-dimethylaminopyridine (DMAP) to afford **6** in 90% overall yield. Thioether formation of **6** with 1-amino-2-methylpropane-2-thiol was accomplished according to a reported condition,

yielding the free amine **7** in 95% yield.[30] Amide-forming reaction of **7** with Cbz-D-Leu-OH under Glyceroacetonide-Oxyma, EDCI, and $NaHCO_3$ in DMF-H_2O[31,32] followed by hydrogenation and deprotection of the Cbz group furnished UT-800 (**1**) in 72% overall yield. Amide-forming reaction of **7** with Boc-D-Leu-OH followed by deprotection of the Boc group furnished **2**•TFA, which was desalted with $NaHCO_3$ in MeOH-H_2O to afford UT-820 (**4**) in 69% overall yield. Similarly, UT-815 (**3**) and UT-810 (**2**) were synthesized in 46-71% overall yields from pleuromutilin (**5**). The analogues (**1**-**4**) synthesized in Scheme 1 were purified via reverse-phase HPLC.

2.3. *In vitro* assays for pleuromutilin analogues 1-4.

The resynthesized molecules **1**-**4** were evaluated in the growth inhibitory assays in both replicating and non-replicating Mtb ($H_{37}Rv$) in microplate alamar blue assay (MABA) and low-oxygen recovery assay (LORA), respectively.[33] The analogs **1**-**4** exhibited the MIC values of 0.78-3.06 μg/mL in MABA. Significantly, **1**-**4** killed non-replicating Mtb at the same level of MIC (1.04 - 3.46 μg/mL). The ratio of MIC_{LORA}/MIC_{MABA} for the three compounds was between 1.13 - 1.45 which is close to the ideal value of 1.0 (Table 1). Because the new analogues **1**-**4** are analogous to valnemulin (Figure 1), antimycobacterial activity of valunemulin was examined and these data are included in Table 1. UT-800 (**1**) and UT-815 (**3**) are the most effective antimycobacterial pleuromutilin analogues identified in our laboratory. To the best of our knowledge, effectiveness of pleuromutilin derivatives against non-replicating Mtb has never been discussed previously. The data summarized in Table 1 may indicate that pleuromutilin can be engineered to be strong anti-TB drugs that are effective against replicating and non-replicating (dormant) forms. The analogues **1**-**4** completely inhibited the coupled transcription/translation reactions (Promega Corporation) at 0.5 μg/mL concertation. In these assays, the IC_{50} values of **1** and linezolid were 0.09 and 0.05 μg/mL, respectively (see SI). Thus, alternations of the structure of the C14-side chain and oxidation states of C3- and C12-functinal groups may not change the primary molecular target of the pleuromutilins. The new analogues identified here displayed cytotoxicity against Vero cells with the IC_{50} values of 25-35 μg/mL.[34] This IC_{50} level was slightly higher than that of valunemulin, however, the selectivity index (defined by IC_{50}/MIC) of **1** and **3** was increased 5-fold relative to that of valunemulin. The analogues **1**-**3** did not induce hemolysis (IC_{50} >200 μM), whereas, tunicamycin (a positive control) lysed the blood cells with IC_{50} of 15.0 μM.

2.4. *In vitro* metabolic stability of the analogues 1-4.

We have reported that *in vitro* half-life ($t_{1/2}$) of valunemulin in rat liver microsomes is significantly extended by reduction of the C3-carbonyl group of valnemulin.[30] Thus, it is interesting to examine metabolic stability of the analogues **1**-**3**. In rat microsomal stability assays, we observed a clear difference in $t_{1/2}$ between **1** and **3**; $t_{1/2}$ of **3** was less than 5 min., on the other hand, $t_{1/2}$ of **1** was >60 min. A C3-carbonyl analogue **2** was also metabolized completely within 10 min (Figure 3). Because of longer $t_{1/2}$ in these assays, UT-800 (**1**) was chosen to evaluate in the basic pharmacological assays (*vide infra*).

2.5. Bactericidal effect of UT-800 (1) against Mtb H37Rv.

The time-kill experiments were performed at two-fold the MIC of UT-800 (**1**), UT-810 (**2**), UT-815 (**3**) and two first-line TB drugs (RIF and INH). Viable cell counting (CFUs) was performed at every 24 h for 14 days. The rate of killing of **1**-**3** against Mtb was compared with the reference molecules; the time-kill assessments at 2xMIC concentrations are summarized in Figure 4. The analogues **1**-**3** killed 100% of Mtb at 2xMIC within 12 days. The observed killing profile of **1**-**3** was similar to that of RIF and INH.

2.6. Effectiveness of UT-800 (1) against intracellular Mtb

The activity of UT-800 (**1**) against intracellular Mtb was evaluated. Murine macrophage cells (J774A.1) infected by the transformant Mtb CDC1551 containing tdTomato (MOI = 10) were treated with **1** (at 2xMIC).[35] After 24, 48, 72, and 96 h of incubation, the relative intensity of the fluorescence was measured (emission wavelength (581 nm)) via fluorescence spectroscopy (Figure 5a). Alternatively, the lysates were ten-fold serially diluted in 7H10-S broth and inoculated on 7H11-S plates to determine the number of viable Mtb cells to confirm the bactericidal effect of **1** in 0-72h (Figure 5b). UT-800 (**1**) killed Mtb in infected macrophages at 2xMIC concentrations within 72 h. The kill-curve of INH, RIF, and **1** in Figure 5a indicate that **1** killed intracellular Mtb more effectively than INH and RIF; bactericidal effect of **1** was distinguished from that of RIF at 48 h. In these experiments, INH did not kill intracellular Mtb at 2xMIC.

2.7. Caco-2 permeability of UT-800 (1).

The pleuromutilin analogue **1** exhibited permeability across Caco-2 epithelial monolayers (*P*app rate coefficient of 3.39×10^{-6} cm/s^{-1}) with moderate levels of efflux (*P*app 18.3×10^{-6} cm/s^{-1}).[36] An efflux ratio of 5.44 indicated that **1** has slightly better membrane permeability than ranitidine (a low permeable control, Table 2).

2.8. Pharmacokinetic property of UT-800 (1).

Pharmacokinetic (PK) data for UT-800 (**1**) were obtained using three and six mice for intravenous (IV) and oral (PO) administration, respectively; PK data of **1** after a single dose (3 mg/kg for IV and 30 mg/kg for PO are summarized in Table 3a and 3b. These data were generously provided by The Global Alliance for TB Drug Development (TB Alliance). An *in vivo* $t_{½}$ of **1** was 9.98 h at a dose of 3 mg/kg (IV). The maximum serum concentration (C_{max}) was 1,908 ng/mL after IV administration. After PO administration, C_{max} was 1,344 ng/mL with t_{max} of 0.83 h. In these preliminary PK studies, the area under the plasma drug concentration-time curve ($AUC_{0\text{-}24h}$) was nearly the same as $AUC_{0\text{-}inf}$, indicating that increasing the dose of **1** may result in an approximately proportional increase in AUC in mice. The 3.3-fold increase in dose of **1** from 3 to 10 mg/kg resulted in a near proportional increase in $AUC_{0\text{-}24h}$ (Table 3a vs 3c) from 993 to 2,497 ng•h/mL. Half-life ($t_{1/2}$) of **1** at dose of 10 mg/kg was not increased prominently compared to that of 3 mg/kg. C_{max} at dose of 10 mg/kg was increased about three-fold. The PK parameters in serum following after a single oral dose of **1** (30 mg/kg) indicated that the peak concentration was reached within 1h after. UT-800 (**1**) was determined to have a bioavailability with the F_{po} of 27.6% in mice (Table 3b). Most importantly, **1** can appropriately be distributed to the lung tissue in mice

(Table 3c). Based on these PK studies, sufficient drug exposure (>MIC of **1**) may be reached in plasma and lungs when sufficient amount of **1** is administered. UT-800 (**1**) displayed a good water solubility (104.7 mg/mL). Acute maximum tolerated doses (MTD) were determined to be 30-40 mg/kg (IV) and >200 mg/kg (PO), respectively. Although much detailed PK studies are required to conclude the potential application of **1** as an oral TB drug lead, theses PK parameters summarized in Table 3 and acceptable MTD values encouraged us to evaluate **1** in an infected mouse model via oral route.

2.9. *In vivo* activity of 1 in the BALB/c acute infection model.

The therapeutic efficacy of **1** was evaluated against Mtb Erdman strain using the BALB/c acute infection model.[37] The treatment of the infected mice (a group of 5 BALB/c female mice, average 19-20 g) with **1** (in water via gavage) was started 10 days later after aerosol infection (Mtb Erdman 2×10^6 CFU). Treatment was continued for three weeks (dosages: 50, 100, and 200 mg/kg). Efficacy in this model was measured as reduction in total lung burdens relative to an untreated control (Table 4). Isoniazid (INH) (at 2.5 mg/kg for 3 weeks) in the BALB/c mouse model reduced the bacterial load by about 4 Log_{10} CFU in lungs. On the other hand, there was no noticeable difference in the number of viable cells in lungs between groups of administration of **1** at doses of 50 mg/kg (~1.0 mg/mouse) and control (vehicle). Although a significant therapeutic efficacy was not observed in the *in vivo* studies (Table 4), **1** showed weak activity in concentration dependent manner; at doses of 200 mg/kg (~4.0 mg/mouse), 0.47 Log_{10} reduction in bacterial burdens was observed ($P < 0.05$), although 5.6-5.7 log_{10} cfu/mouse of viable organisms persisted.

3. Conclusion

In our discovery program for identification of new pleuromutilin derivatives against Gram-negative bacteria, we have generated a library of pleuromutilin derivatives. Here, we describe our discovery of several antimycobacterial analogues identified in our library molecules. UT-800 (**1**) exhibits a strong antibacterial activity against replicating and non-replicating Mtb with the MIC_{LORA}/MIC_{MABA} ration of 1.45. As observed in our anti-*Acinetobacter* analogues,[30] a C3-hydroxy analogue **1** shows longer half-life in the rat microsomes than the other analogues possessing the C3-carbonyl group (e.g. valnemulin). Bactericidal activity of **1** against intracellular Mtb highlights uniqueness of antimycobacterial pleuromutilin derivatives. Pharmacokinetic parameters of **1** indicates that **1** has oral bioavailability and is distributed to the lung tissues in mice. Although the PK property of the selected analogue **1** is far from that of ideal TB drugs, it is very interesting to investigate whether **1** is effective in an infected mouse model via oral administration. In an acute efficacy studies using infected BALB/c mice, **1** showed ~0.5 log_{10} reduction of Mtb burden in the lungs. The results summarized in this article can conclude that the improvements of therapeutic window by reducing toxicity level and PK property are essential for the current lead to be an oral TB drug candidate.

4. Experimental section

4.1. Chemical synthesis

4.1.1. General experimental methods—All chemicals were purchased from commercial sources and used without further purification unless otherwise noted. THF, CH_2Cl_2, and DMF were purified via Innovative Technology's Pure-Solve System. All reactions were performed under an Argon atmosphere. All stirring was performed with an internal magnetic stirrer. Reactions were monitored by TLC using 0.25 mm coated commercial silica gel plates (EMD, Silica Gel $60F_{254}$). TLC spots were visualized by UV light at 254 nm, or developed with ceric ammonium molybdate or anisaldehyde or copper sulfate or ninhydrin solutions by heating on a hot plate. Reactions were also monitored by using SHIMADZU LCMS-2020 with solvents: A: 0.1% formic acid in water, B: acetonitrile. Flash chromatography was performed with SiliCycle silica gel (Purasil 60 Å, 230-400 Mesh). Proton magnetic resonance (^{1}H-NMR) spectral data were recorded on 400, and 500 MHz instruments. Carbon magnetic resonance (^{13}C-NMR) spectral data were recorded on 100 and 125 MHz instruments. For all NMR spectra, chemical shifts (δH, δC) were quoted in parts per million (ppm), and *J* values were quoted in Hz. ^{1}H and ^{13}C NMR spectra were calibrated with residual undeuterated solvent ($CDCl_3$: δH = 7.26 ppm, δC = 77.16 ppm; CD_3CN: δH = 1.94 ppm, δC = 1.32ppm; CD_3OD: δH =3.31 ppm, δC =49.00 ppm; DMSO-d_6: δH = 2.50 ppm, δC = 39.52 ppm; D_2O: δH = 4.79 ppm) as an internal reference. The following abbreviations were used to designate the multiplicities: s = singlet, d = doublet, dd = double doublets, t = triplet, q = quartet, quin = quintet, hept = heptet, m = multiplet, br = broad. Infrared (IR) spectra were recorded on a Perkin-Elmer FT1600 spectrometer. HPLC analyses were performed with a Shimadzu LC-20AD HPLC system. All compounds were purified by reverse HPLC to be ≥95% purity.

4.1.2. Synthesis of 1—The amino-alcohol **7** was synthesized according the procedure described previously.[30] To a stirred solution of **7** (1.51 g, 3.22 mmol), Cbz-D-Leu-OH (1.28 g, 4.83 mmol), $NaHCO_3$ (2.70 g, 32.2 mmol) and Glyceroacetonide-Oxyma (1.10 g, 4.83 mmol) in DMF-H_2O (9/1, 16 mL) was added EDCI (3.08 g, 16.1 mmol). The reaction mixture was stirred for 2h at rt, quenched with aq. sat. $NaHCO_3$, and extracted with EtOAc. The combined organic extract was washed with 1*N* HCl, brine, dried over Na_2SO_4 and concentrated *in vacuo*. The crude mixture was purified by silica gel column chromatography (hexanes/EtOAc 60:40 to 25:75) to afford **8** (2.04 g, 2.86 mmol, 88%). To a stirred solution of **8** (1.50 g, 2.10 mmol) in MeOH/EtOAc (1:1, 210 mL) was added Pd/C (10 wt %, 900 mg). H_2 gas was introduced and the reaction mixture was stirred for 120 h under H_2. The solution was filtered through Celite and concentrated in vacuo. The crude mixture was purified by silica gel column chromatography ($CHCl_3$/MeOH 95:5 to 90:10) to afford **1** (1.01 g, 1.73 mmol, 82%). UT-800 (**1**) was purified by C18 reverse-phase HPLC [column: HYPERSIL GOLD™ (175 Å, 12 μm, 250 × 10 mm), solvents: a gradient elution of 25:75 to 55:45 MeOH : H_2O over 20 min then 55:45 MeOH : H_2O, flow rate: 2.0 mL/min, UV: 220 nm, retention time: 25 min]: TLC ($CHCl_3$/MeOH 90:10) R_f = 0.30; $[\alpha]^{21}_D$ +0.004 (*c* = 0.81, MeOH); IR (thin film) ν_{max} = 3432 (br), 2958, 2876, 1680, 1562, 1464, 1370, 1290, 1144, 1020, 1001, 970, 930 cm^{-1}; ^{1}H NMR (400 MHz, Methanol-d_4) δ 5.58 (d, *J* = 9.0 Hz, 1H), 4.48 (t, *J* = 5.6 Hz, 1H), 3.94 (dd, *J* = 8.2, 5.6 Hz, 1H), 3.38 (dd, *J* = 14.8, 4.5 Hz, 2H), 3.35

(s, 2H), 3.29 – 3.23 (m, 2H), 2.36 (tq, *J* = 11.2, 7.0, 5.6 Hz, 1H), 2.17 (quin, *J* = 6.8 Hz, 1H), 1.94 (dd, *J* = 12.9, 3.7 Hz, 1H), 1.91 – 1.86 (m, 1H), 1.84 – 1.73 (m, 4H), 1.73 – 1.64 (m, 3H), 1.64 – 1.56 (m, 2H), 1.52 (dd, *J* = 14.1, 7.4 Hz, 1H), 1.48 – 1.41 (m, 1H), 1.41 – 1.35 (m, 1H), 1.35 – 1.32 (m, 1H), 1.30 (s, 3H), 1.28 (s, 3H), 1.23 (s, 3H), 1.05 (d, *J* = 4.8 Hz, 3H), 1.04 (d, *J* = 4.9 Hz, 3H), 0.91 (s, 3H), 0.86 (d, *J* = 7.0 Hz, 3H), 0.74 (t, *J* = 7.4 Hz, 3H), 0.69 (d, *J* = 7.2 Hz, 3H); ^{13}C NMR (101 MHz, MeOD) δ 172.24, 170.72, 77.33, 77.17, 73.47, 53.14, 52.19, 47.83, 47.17, 42.66, 42.55, 42.04, 42.01, 37.20, 35.42, 34.59, 33.16, 32.66, 32.44, 29.06, 26.95, 26.91, 26.68, 25.56, 23.13, 22.19, 21.47, 17.77, 17.54, 12.52, 8.79; HRMS (ESI+) *m*/*z* calcd for $C_{32}H_{59}N_2O_5S$ [M + H] 583.4145, found: 583.4166.

4.1.3. Tosylation of pleuromutilin (5)—To a stirred solution of **5** (2.00 g, 5.28 mmol) in CH_2Cl_2 (26.4 mL) was added TsCl (1.21 g, 6.34 mmol) and DMAP (1.94 g, 15.9 mmol) at 0 °C. After 4h at 0 °C, the reaction mixture was quenched with 1*N* HCl and extracted with EtOAc. The combined organic extract was washed with aq. sat. $NaHCO_3$, dried over Na_2SO_4, concentrated *in vacuo*. The crude product was purified by silica gel column chromatography (hexanes/EtOAc 60:40) to yield **10** (2.13 g, 3.99 mmol, 76%): TLC (hexanes/EtOAc 50:50) R_f = 0.50; $[\alpha]^{20}_D$ +0.355 (*c* = 1.81, $CHCl_3$); IR (thin film) ν_{max} = 3566 (br), 2984, 2937, 2883, 2865, 1757, 1732, 1598, 1455, 1368, 1291, 1223, 1190, 1176, 1117, 1096, 1038, 1019, 815, 753, 719, 663 cm^{-1}; ^{1}H NMR (400 MHz, Chloroform-*d*) δ 7.80 (d, *J* = 8.4 Hz, 2H), 7.35 – 7.32 (m, 2H), 6.39 (dd, *J* = 17.4, 11.0 Hz, 1H), 5.75 (d, *J* = 8.5 Hz, 1H), 5.31 (dd, *J* = 11.0, 1.5 Hz, 1H), 5.17 (dd, *J* = 17.4, 1.6 Hz, 1H), 4.46 (s, 2H), 3.33 (dd, *J* = 10.5, 6.5 Hz, 1H), 2.44 (s, 3H), 2.29 – 2.13 (m, 3H), 2.08 – 2.05 (m, 1H), 2.01 (d, *J* = 8.7 Hz, 1H), 1.74 (dq, *J* = 14.4, 3.0 Hz, 1H), 1.68 – 1.58 (m, 1H), 1.53 – 1.41 (m, 2H), 1.39 (s, 3H), 1.36 – 1.33 (m, 1H), 1.33 – 1.27 (m, 1H), 1.23 (d, *J* = 15.9 Hz, 1H), 1.14 (s, 3H), 1.08 (dd, *J* = 13.9, 4.5 Hz, 1H), 0.86 (d, *J* = 6.9 Hz, 3H), 0.61 (d, *J* = 7.0 Hz, 3H); ^{13}C NMR (101 MHz, $CDCl_3$) δ 216.63, 164.81, 145.24, 138.70, 132.60, 129.87 (2C), 128.04 (2C), 117.29, 74.49, 70.27, 65.01, 57.98, 45.35, 44.48, 43.94, 41.81, 36.51, 36.00, 34.36, 30.30, 26.74, 26.39, 24.78, 21.64, 16.48, 14.72, 11.42; HRMS (ESI+) *m*/*z* calcd for $C_{29}H_{41}O_7S$ [M + H] 533.2573, found: 533.2546.

4.1.4. Synthesis of 11—To a stirred solution of **10** (196 mg, 0.37 mmol), 1-amino-2-methylpropane-2-thiol hydrochloride (104 mg, 0.74 mmol) and *tetra*-*n*-butylammonium bromide (11.9 mg, 0.037 mmol) in THF (1.5 mL) was added 1*N* NaOH (1.5 mL). After 3h at 50 °C, the reaction mixture was extracted with $CHCl_3$. The combined organic extract was dried over Na_2SO_4, concentrated *in vacuo*. The crude product was purified by silica gel column chromatography (hexanes/EtOAc 50:50 to $CHCl_3$/MeOH 75:25) to give **11** (140 mg, 0.30 mmol, 82%): TLC ($CHCl_3$/MeOH 90:10) R_f = 0.20; $[\alpha]^{20}_D$ +0.335 (*c* = 1.49, $CHCl_3$); IR (thin film) ν_{max} = 3433 (br), 2928, 2881, 2864, 1726, 1631, 1524, 1457, 1412, 1375, 1281, 1152, 1119, 1033, 1010, 980, 954, 938, 916, 816, 754, 683 cm^{-1}; ^{1}H NMR (400 MHz, Chloroform-*d*) δ 6.48 (dd, *J* = 17.4, 11.0 Hz, 1H), 5.76 (d, *J* = 8.4 Hz, 1H), 5.36 (dd, *J* = 10.9, 1.5 Hz, 1H), 5.21 (dd, *J* = 17.4, 1.6 Hz, 1H), 3.36 (d, *J* = 6.5 Hz, 1H), 3.15 (d, *J* = 2.3 Hz, 2H), 2.63 (s, 2H), 2.38 – 2.30 (m, 1H), 2.32 – 2.14 (m, 2H), 2.13 – 2.03 (m, 2H), 1.87 (brs, 2H), 1.77 (dq, *J* = 14.4, 3.1 Hz, 1H), 1.71 – 1.61 (m, 2H), 1.60 – 1.50 (m, 2H), 1.50 – 1.47 (m, 1H), 1.46 (s, 3H), 1.41 – 1.33 (m, 1H), 1.26 (s, 6H), 1.17 (s, 3H), 1.11 (dd, *J* = 14.0, 4.3 Hz, 1H), 0.88 (d, *J* = 7.0 Hz, 3H), 0.73 (d, *J* = 6.9 Hz, 3H); ^{13}C NMR (101 MHz,

$CDCl_3$) δ 216.94, 169.57, 139.01, 117.30, 74.64, 69.52, 58.21, 51.42, 48.22, 45.47, 44.78, 43.95, 41.82, 36.79, 36.03, 34.46, 31.32, 30.46, 26.87, 26.34, 26.33, 26.29, 24.87, 16.86, 14.92, 11.50; HRMS (ESI+) *m/z* calcd for $C_{26}H_{44}NO_4S$ [M + H] 466.2991, found: 466.3016.

4.1.5. Synthesis of 2—To a stirred solution of **11** (62.1 mg, 0.13 mmol), Boc-D-Leu-OH (46.2 mg, 0.20 mmol), $NaHCO_3$ (112 mg, 1.33 mmol) and Glyceroacetonide-Oxyma (45.6 g, 1.20 mmol) in DMF-H_2O (9/1, 0.7 mL) was added EDCI (128 mg, 0.67 mmol). The reaction mixture was stirred for 5h at rt, quenched with aq. sat. $NaHCO_3$, and extracted with EtOAc. The combined organic extract was washed with 1*N* HCl, brine, dried over Na_2SO_4 and concentrated *in vacuo*. The crude mixture was purified by silica gel column chromatography (hexanes/EtOAc 75:25 to 60:40) to afford **12** (55.2 mg, 0.081 mmol, 61%). To a stirred solution of **12** (18.7 mg, 0.027 mmol) in dioxane (0.2 mL) was added a 4*N* solution of HCl in dioxane (0.8 mL). The reaction mixture was stirred for 1h at rt, and all volatiles were evaporated *in vacuo*. The crude mixture was basified with $NaHCO_3$ in MeOH and purified by C18 reverse-phase HPLC [column: HYPERSIL GOLD™ (175 Å, 12 μm, 250 × 10 mm), solvents: a gradient elution of 70:30 to 100:0 MeOH : H_2O over 20 min, flow rate: 2.0 mL/min, UV: 220 nm] to afford **2** (11.9 mg, 0.021 mmol, 75%, retention time: 18 min): TLC ($CHCl_3$/MeOH 90:10) R_f = 0.20; $[\alpha]^{21}_D$ +0.125 (*c* = 0.50, MeOH); IR (thin film) ν_{max} = 3354 (br), 2955, 2932, 2867, 1729, 1659, 1522, 1464, 1414, 1386, 1368, 1282, 1144, 1117, 1019, 981, 953, 939, 917 cm^{-1}; ^1H NMR (400 MHz, Methanol-d_4) δ 6.32 (dd, *J* = 17.9, 10.8 Hz, 1H), 5.75 (d, *J* = 8.3 Hz, 1H), 5.17 (q, *J* = 1.6 Hz, 1H), 5.14 (q, *J* = 1.6 Hz, 1H), 3.50 (d, *J* = 6.1 Hz, 1H), 3.39 (dd, *J* = 8.2, 6.1 Hz, 1H), 3.28 (d, *J* = 5.9 Hz, 2H), 2.39 – 2.32 (m, 2H), 2.32 – 2.22 (m, 1H), 2.16 (ddd, *J* = 16.0, 8.9, 4.9 Hz, 2H), 1.85 – 1.79 (m, 1H), 1.76 (ddd, *J* = 13.1, 6.6, 1.5 Hz, 1H), 1.69 (dt, *J* = 11.2, 2.2 Hz, 1H), 1.66 – 1.54 (m, 4H), 1.48 (d, *J* = 2.6 Hz, 1H), 1.46 (s, 3H), 1.44 – 1.32 (m, 4H), 1.32 – 1.28 (m, 1H), 1.27 (s, 3H), 1.25 (s, 3H), 1.15 (s, 3H), 0.98 (d, *J* = 6.6 Hz, 3H), 0.95 (d, *J* = 6.5 Hz, 3H), 0.93 (d, *J* = 7.0 Hz, 3H), 0.73 (d, *J* = 6.6 Hz, 3H); ^{13}C NMR (101 MHz, MeOD) δ 219.60, 178.24, 171.39, 141.16, 116.62, 75.46, 71.45, 59.32, 54.73, 47.81, 47.79, 47.77, 46.81, 45.99, 45.76, 45.25, 43.14, 38.16, 37.72, 35.29, 31.52, 28.17, 28.05, 26.90, 26.79, 25.92, 25.85, 23.47, 22.52, 17.13, 15.41, 11.77; HRMS (ESI+) *m/z* calcd for $C_{32}H_{55}N_2O_5S$ [M + H] 579.3832, found: 579.3864.

4.1.6. Synthesis of 3—To a stirred solution of **11** (0.24 g, 0.51 mmol), Cbz-D-Leu-OH (0.20 g, 0.76 mmol), $NaHCO_3$ (0.43 g, 5.08 mmol) and Glyceroacetonide-Oxyma[2] (0.17 g, 0.76 mmol) in DMF-H_2O (9/1, 2.54 mL) was added EDCI (0.49 g, 2.54 mmol). The reaction mixture was stirred for 1h at rt, quenched with aq. sat. $NaHCO_3$, and extracted with EtOAc. The combined organic extract was washed with 1*N* HCl, brine, dried over Na_2SO_4 and concentrated *in vacuo*. The crude mixture was purified by silica gel column chromatography (hexanes/EtOAc 60:40 to 25:75) to afford **13** (0.33 g, 0.46 mmol, 91%). To a stirred solution of **13** (11.7 mg, 0.016 mmol) in MeOH/EtOAc (1:1, 3.0 mL) was added Pd/C (10 wt %, 5.0 mg). H_2 gas was introduced and the reaction mixture was stirred for 20 h under H_2. The solution was filtered through Celite and concentrated *in vacuo*. The crude mixture was purified by C18 reverse-phase HPLC [column: HYPERSIL GOLD™ (175 Å, 12 μm, 250 × 10 mm), solvents: a gradient elution of 25:75 to 55:45 MeOH : H_2O over 20 min then 55:45

MeOH : H_2O, flow rate: 2.0 mL/min, UV: 220 nm] to afford **3** (7.5 mg, 0.013 mmol, 78%, retention time: 29 min): TLC ($CHCl_3$/MeOH 90:10) R_f = 0.20; $[\alpha]^{21}_D$ +0.071 (*c* = 0.27, MeOH); IR (thin film) ν_{max} = 3344 (br), 2958, 2932, 2871, 1732, 1664, 1521, 1464, 1384, 1368, 1282, 1148, 1117 cm^{-1}; ^1H NMR (400 MHz, Methanol-d_4) δ 5.67 (d, *J* = 8.2 Hz, 1H), 3.45 (d, *J* = 6.0 Hz, 1H), 3.39 (dd, *J* = 8.2, 6.1 Hz, 1H), 3.35 (s, 1H), 3.29 (d, *J* = 3.2 Hz, 1H), 2.41 – 2.31 (m, 2H), 2.26 (dddd, *J* = 19.3, 11.1, 2.6, 1.3 Hz, 1H), 2.14 (dt, *J* = 19.2, 9.3 Hz, 1H), 1.85 – 1.72 (m, 4H), 1.69 (dt, *J* = 11.2, 2.1 Hz, 1H), 1.65 – 1.49 (m, 5H), 1.47 (d, *J* = 2.5 Hz, 1H), 1.45 (s, 3H), 1.40 (d, *J* = 1.2 Hz, 1H), 1.39 – 1.32 (m, 3H), 1.28 (s, 3H), 1.26 (s, 3H), 1.14 (td, *J* = 14.2, 4.6 Hz, 1H), 0.98 (d, *J* = 6.6 Hz, 3H), 0.96 (d, *J* = 6.5 Hz, 3H), 0.94 (s, 3H), 0.91 (s, 3H), 0.74 (t, *J* = 7.4 Hz, 3H), 0.73 (d, *J* = 6.8 Hz, 3H); ^{13}C NMR (101 MHz, MeOD) δ 219.67, 178.22, 171.80, 76.65, 71.41, 59.40, 54.73, 47.86, 47.84, 46.84, 45.78, 43.07, 41.94, 41.72, 38.16, 35.90, 35.29, 32.31, 31.46, 28.15, 26.88, 26.78, 26.74, 25.93, 25.70, 23.48, 22.51, 21.44, 17.30, 15.43, 11.71, 8.81; HRMS (ESI+) *m*/*z* calcd for $C_{32}H_{57}N_2O_5S$ [M + H] 581.3988, found: 581.3958.

4.1.7. Synthesis of 4—To a stirred solution of **7** (83.1 mg, 0.18 mmol), Boc-D-Leu-OH (61.6 mg, 0.27 mmol), $NaHCO_3$ (149 mg, 1.78 mmol) and Glyceroacetonide-Oxyma (60.8 mg, 0.27 mmol) in DMF-H_2O (9/1, 0.9 mL) was added EDCI (170 mg, 0.89 mmol). The reaction mixture was stirred for 5h at rt, quenched with aq. sat. $NaHCO_3$, and extracted with EtOAc. The combined organic extract was washed with 1*N* HCl, brine, dried over Na_2SO_4 and concentrated *in vacuo*. The crude mixture was purified by silica gel column chromatography (hexanes/EtOAc 67:33 to 60:40) to afford **9** (108 mg, 0.158 mmol, 89%). To a stirred solution of **9** (27.2 mg, 0.040 mmol) in dioxane (0.2 mL) was added a 4*N* solution of HCl in dioxane (0.4 mL). The reaction mixture was stirred for 1h at rt, and all volatiles were evaporated *in vacuo*. The crude mixture was basified with $NaHCO_3$ in MeOH, and purified by C18 reverse-phase HPLC [column: HYPERSIL GOLD™ (175 Å, 12 μm, 250 × 10 mm), solvents: a gradient elution of 70:30 to 100:0 MeOH : H_2O over 20 min, flow rate: 2.0 mL/min, UV: 220 nm] to afford **4** (18.1 mg, 0.031 mmol, 78%, retention time: 17 min): TLC ($CHCl_3$/MeOH 90:10) R_f = 0.20; ^1H NMR (400 MHz, Methanol-d_4) δ 6.38 – 6.27 (m, 1H), 5.87 (d, *J* = 8.2 Hz, 1H), 5.14 (dq, *J* = 14.1, 1.6 Hz, 2H), 3.80 (s, 3H), 3.41 (d, *J* = 6.1 Hz, 1H), 3.40 – 3.38 (m, 1H), 3.29 – 3.26 (m, 2H), 2.59 (s, 1H), 2.50 (dtd, *J* = 19.2, 9.6, 1.2 Hz, 1H), 2.31 (ddt, *J* = 18.5, 9.7, 7.4 Hz, 2H), 2.22 (dd, *J* = 14.5, 6.9 Hz, 1H), 2.08 – 1.96 (m, 1H), 1.76 (ddt, *J* = 13.1, 7.7, 6.5 Hz, 1H), 1.67 (dt, *J* = 13.6, 2.7 Hz, 1H), 1.63 – 1.55 (m, 2H), 1.50 (s, 3H), 1.49 – 1.47 (m, 1H), 1.46 – 1.42 (m, 1H), 1.42 – 1.38 (m, 1H), 1.36 (d, *J* = 5.1 Hz, 1H), 1.33 – 1.31 (m, 1H), 1.31 – 1.28 (m, 1H), 1.27 (s, 3H), 1.25 (s, 3H), 1.20 (d, *J* = 4.5 Hz, 1H), 1.15 (s, 3H), 0.98 (d, *J* = 6.6 Hz, 3H), 0.96 (d, *J* = 6.6 Hz, 3H), 0.89 (d, *J* = 7.0 Hz, 3H), 0.73 (d, *J* = 7.2 Hz, 3H); ^{13}C NMR (101 MHz, MeOD) δ 178.03, 171.47, 167.64, 141.28, 116.51, 75.36, 72.09, 61.77, 54.70, 53.81, 47.81, 45.99, 45.68, 45.15, 43.63, 37.81, 36.36, 32.51, 30.48, 28.72, 28.30, 28.11, 26.91, 26.79, 25.92, 24.67, 23.47, 22.51, 17.19, 17.18, 12.84; HRMS (ESI+) *m*/*z* calcd for $C_{32}H_{57}N_2O_5S$ [M + H] 581.3988, found: 581.3976.

4.2. Biological assays

4.2.1. Bacterial culture conditions—A single colony of each *Mycobacterium* strain (*M. tuberculosis* H_{37}Rv was obtained on a Difco Middlebrook 7H10 nutrient agar enriched

with 10% oleic acid, albumin, dextrose and catalase (OADC). Seed cultures of each *Mycobacterium* strain were obtained in Middlebrook 7H9 broth enriched with OADC. Flasks containing each bacterial strain was incubated to mid-log phase in their respective culture media, in a shaking incubator at 37 °C with a shaking speed of 200 rpm and cultured to mid-log phase (Optical density - 0.5). The optical density was monitored at 600 nm using a microplate reader (Biotek Synergy XT).

4.2.2. Minimum inhibitory concentration (MIC) assays

4.2.2.1. Microplate alamar blue assay (MABA): These were performed according to the published protocol.[38] Bacterial cultures at 0.5 optical density, was treated with serial dilutions of inhibitors in aerobic conditions and incubated at 37 °C for 15 days for *M. tuberculosis* (H37Rv) and *M. bovis* (BCG). Incubation time was 48h for *M. smegmatis* (ATCC 607). All other bacteria were incubated for 24 h. After incubation, 20 μL of resazurin (stock-0.02%) was added and incubated on a shaking incubator at 37 °C for 4 h for *M.tuberculosis* and *M. bovis*. For all other bacteria 20 μL was added from a 0.08% resazurin stock solution and left for 1 h. The lowest concentration at which the color of resazurin was completely retained as blue was read as the MIC_{100} (Pink = Growth, Blue = No growth). The absorbance measurements were also performed using a Biotek Synergy XT (Winooski, VT, USA), 96 well plate reader at 570 nm and 600 nm. Assay plates for *C. difficile* was incubated for 24 h in the anaerobic conditions and the optical density was measured at the end of incubation and wells with no visible growth was considered MIC.

4.2.2.2. Luminescence-based low-oxygen-recovery assay (LORA): These assays were performed according to the reported procedures.[33] In brief, *M. tuberculosis* H37Rv cells were transformed by mixing at least 1 μg of the purified plasmid, pFCA-luxAB and incubating at room temperature for 30 min, followed by electroporation.[39] *M.tuberculosis* pFCA-luxAB strain cultured was diluted in Middlebrook 7H12 broth, and sonicated for 15s. The cultures were diluted to obtain an A570 of 0.03 to 0.05 and 3,000 to 7,000 RLUs per 100 μl. Two-fold serial dilutions of antimicrobial agents were prepared in black 96-well microtiter plates (100 μl), and 100 μl of the cell suspension was added. The microplate was placed under anaerobic conditions (oxygen concentration, less than 0.16%) by using an Anoxomat model WS-8080 (MART Microbiology) and three cycles of evacuation and filling with a mixture of 10% H_2, 5% CO_2, and 85% N_2. Incubation was continued for 10 days, and transferred to an ambient gaseous condition (5% CO_2-enriched air) incubator for a 28h "recovery." 100 μl culture was transferred to white 96-well microtiter plates for determination of luminescence.

4.2.3. Cytotoxicity assays—Selected molecules were tested for cytotoxicity (IC_{50}) in Vero cells via a MTT colorimetric assay. Vero cell line was cultured in Complete eagle's minimum essential growth medium (EMEM) containing L-glutamine, sodium pyruvate, minimum essential amino acids, penicillin-streptomycin and 10% fetal bovine serum. After 72h of exposure of molecules to this cell line at concentrations ranging from 0.78 to 200 μg/mL, the culture medium was changed to complete EMEM without phenol red before addition of yellow tetrazolium dye; MTT. Viability was assessed on the basis of cellular

conversion of MTT into a purple formazan product. The absorbance of the colored formazan product was measured at 570 nm by BioTek Synergy HT Spectrophotometer.

4.2.4. Killing Effect against intracellular Mtb—J774A.1 cells were seeded at 2.5 × 10^5 cells/well in 24-well dishes or 1 × 10^5 cells/well in 8-well chamber slides and incubated overnight at 37 °C in DMEM. A transformant *M. tuberculosis* CDC1551 expressing tdTomato was grown in 7H9 Middlebrook medium supplemented with OADC. The Mtb cells were harvested at an optical density of 0.5, washed and re-suspended in saline. J774A.1 cells were maintained in cell culture medium and were infected by Mtb (10^6 bacteria in 0.2 mL of media): a multiplicity of infection (MOI) of ≈10 (bacteria/cell).[35] The extracellular bacteria were removed by washing with PBS. The infected macrophages were treated with antibacterial agents at 2xMIC concentrations and the relative intensity of the fluorescence was measured [emission wavelength (581 nm)] via UV–vis spectroscopy in 24, 48, 72, and 96h for inhibition of intracellular bacterial growth. Surviving Mtb cells were confirmed by CFU method.

4.2.5. Kill-curve of Mtb by 1—*M. tuberculosis* H_{37}Rv cultures at mid-log phase (OD = 0.5) were diluted to OD = 0.25 and treated with inhibitor molecules at MIC, 2xMIC and 4x MIC. Each culture well was diluted 10, 100, 1000 and 10,000-fold every 24 h and 20μL from each dilution was plated on 7H10 agar plates supplemented with OADC enrichment. Plates were incubated for 15 days in a static incubator at 37 °C and colonies were counted.

4.2.6. Microsomal stability—Pooled Sprague-Dawley rat liver microsomes were purchased from Corning Life Sciences (Oneonta, NY, USA). Microsomes (20 mg/mL) were thawed on ice and diluted using phosphate buffer (100 mM, pH: 7.4), resulting in a protein concentration of 1 mg/mL. Stock solutions (10 mg/L) of test molecules were prepared in DMSO (50%). A final concentration of 500 ng/mL was used for incubation with microsomes. NADPH (final concentration: 1 mM) was used as a co-factor. All the above solutions except NADPH were added to individual wells (12-well) in triplicate and were allowed to equilibrate for 5 min at 37°C. NADPH was then added. 50 μL aliquots in triplicate were drawn from the incubation mixture at 0, 5, 10, 20, 30, 45 and 60 min and immediately the reaction was quenched by addition of ice-cold methanol (4 volumes). The samples containing methanol was lyophilized to remove all volatiles. The residue was dissolved in 1*N* HCl. (10 μL) and MeOH (40 μL). The resulting solution (20 μL) was quantified via LC-MS. MS solvent: 90:10 acetonitrile/0.05% formic acid in water, flow rate: 0.5mL/min.

4.2.7. Prediction of intestinal permeability of 1 *via* Caco-2 permeability assay —The suitability of **1** for oral dosing was evaluated by using a bidirectional Caco-2 permeability assay by Cyprotex.[40] Test molecue was added to the apical side of the membrane and the transport of the compound across the monolayer was monitored over a 2h time period. The transport of test molecule in the apical to basolateral direction (A-B) as well as the basolateral to apical direction (B-A) was assessed to determine an efflux ratio which provides an indicator as to whether test molecule undergoes active efflux. The permeability coefficient (P_{app}) of **1** was determined to be 3.39 × 10^{-6} cm/s from A-B and

18.3×10^{-6} cm/s from B-A. Efflux ratio (P_{app}(B-A)/P_{app}(A-B)) was determined to be 5.44. Ranitidine was used as a low permeability control ($P_{app} < 1$) and warfarin was used as a high permeability control ($P_{app} > 1$). Talinolol, a known P-gp substrate, was screened as a control compound to confirm that the cells are expressing functional efflux proteins (P_{app}(B-A)/ P_{app}(A-B) = 76.8). A P_{app} rate coefficient > 1 and efflux ratio approximately 5 indicates that **1** has permeability across the membrane with moderate levels of efflux (An efflux ratio greater than two indicates that drug efflux is occurring).

4.2.8. Hemolysis assay—Heparinized whole sheep blood was washed three times with saline (0.9% NaCl) and the pellet was suspended in PBS buffer (150 mM NaCl, 5 mM KCl, 10mM PBS, 2.5mM $CaCl_2$, 10 mM glucose, pH 7.4). 0.5 ml of 3% erythrocytes in PBS buffer, pH 7.4 was treated with test molecule in concentrations ranging from 2-200 μg/mL). Triton X 100 was used as positive control in concentrations 0.01, 0.1 and 1%. As a negative control, 0.5% PEG:H_2O (2:1) (diluent for test compounds) was used in the same concentration as in samples (2.5 μL). The assay mixture was incubated at 37 °C for 2h with gentle shaking. The assay mixture was centrifuged at 4,700 rpm for 5 min and the released hemoglobin in the supernatant was determined at $OD_{540nm.}$ The percentage of hemolysis was calculated from the equation ($100 \times (A_{sample} - A_{negative\ control}) / (A_{positive\ control} - A_{negative\ control})$).[41]

4.2.9. LD_{50} and PK analyses—Animal protocol number (17-026.0-A) was approved by the Institutional Animal Care and Use Committee (IACUC) at the University of Tennessee on 05/30/2017. C57BI male mice aged 7-8 weeks from Jackson labs were used. The mice were injected with **1** using retroorbital injection method under anesthesia. To determine whether **1** exerted any overt toxicity, 3 groups of mice with 6 in each group were injected with increasing doses of **1** (10 mg/kg, 25 mg/kg, and 50 mg/kg), and their health status was monitored over a period of 7 days. The mice were monitored 3 times a day for the first 72h to ensure that the mice did not experience negative health effects due to the administration of the drug. The mice had their blood collected by submandibular bleed on each day after the injection of **1**. At the end of the study period, the mice were sacrificed by cardiac puncture, and the plasma, lungs, kidney, and spleen were collected. Analyses of the plasma and lung sample were performed to determine basic PK parameters (half-life, T_{max}, C_{max}).

4.2.10. *In vivo* activity of 1—Animal protocol number (15-170) was approved by the Institutional Animal Care and Use Committee (IACUC) at the University of Chicago Illinois on 09/15/2017. Efficacy of **1** in killing Mtb Erdman was evaluated in a short-term acute efficacy mouse model. Seven to eight week old female BALB/c mice were infected with Mtb Erdman by aerosol using a glass-col chamber, resulting in the deposition of ~100 CFU in the lungs of individual mice. After 10 days, (50, 100 and 200 mg/kg) of **1** (in water) were administered to groups of 5 female mice. Treatment was continued for three weeks. Mice were humanely euthanized and the lungs and spleens were aseptically harvested for bacterial enumeration at days 21 post-infection. Efficacy was measured as reduction in total lung burdens relative to an untreated control.

4.2.11. Transcription/translation coupled assay—Transcription/translation coupled assays were performed using commercially available *E. coli* S30 circular DNA assay kit (L1020) purchased from Promega Corporation. The assay used a control DNA template, pBESTluc™ vector containing the eukaryotic firefly luciferase gene positioned downstream from the tac promoter and a ribosome binding site. The protein product, luciferase was synthesized from 2μg of pBESTluc™ DNA using 5 uL complete amino acid mixture, 15 uL S30 extract (rNTPs, tRNAs, an ATP-regenerating system, IPTG and appropriate salts) and 20 uL premix provided with the assay kit in a final reaction volume of 50 uL with nuclease free water. Inhibitor compounds were dissolved in DMSO. Assays were setup with a master mix consisting of S30 extract and water, amino acid mix, and the S30 Premix, followed by the addition of test compound. Master mix was dispensed to microcentrifuge tubes and reactions were initiated by the addition of DNA template. Reaction mixture was vortexed gently, centrifuged for 5 sec. and incubated at 37°C for 60 min. Reactions were stopped by placing tubes in ice bath for 5 min. and diluted in two-fold dilution series using 50 uL of luciferase dilution reagent (Promega Corporation) containing luciferase assay substrate, and transferred to 96 well white plate. The luminescence readout was performed immediately with UV-Vis.

Supplementary Material

Refer to Web version on PubMed Central for supplementary material.

Acknowledgements

The National Institutes of Health is greatly acknowledged for financial support of this work (AI084411). We also thank University of Tennessee for generous financial support (CORNET award). NMR data were obtained on instruments supported by the NIH Shared Instrumentation Grant. The authors gratefully acknowledge Drs. Takushi Kaneko (GATB) and Stefan Schweitzer (University of Tennessee Research Foundation) for useful discussions.

References

1. Siricilla S; Mitachi K; Wan B; Franzblau SG; Kurosu M Discovery of a Capuramycin Analog that Kills Non-Replicating *Mycobacterium tuberculosis* and Its Synergistic Effects with Translocase I Inhibitors. J. Antibiot. 2014, 68, 271–278. [PubMed: 25269459]
2. Cooper AM; Flynn JL The Protective Immune Response to Mycobacterium tuberculosis. Curr. Opin. Immunol 1995, 7, 512–516. [PubMed: 7495515]
3. Ramakrishnan L Revisiting the Role of the Granuloma in Tuberculosis. Nat. Rev. Immunol 2012, 12, 352–366. [PubMed: 22517424]
4. Wayne LG; Hayes LG An In Vitro Model for Sequential Study of Shiftdown of Mycobacterium tuberculosis through Two Stages of Nonreplicating Persistence. Infect. Immun 1996, 64, 2062–2069. [PubMed: 8675308]
5. Engohang-Ndong J Antimycobacterial Drugs Currently in Phase II Clinical Trials and Preclinical Phase for Tuberculosis Treatment. Expert Opin. Investig. Drugs. 2012, 21, 1789–1800.
6. Kaneko T; Cooper C; Mdluli K Challenges and opportunities in developing novel drugs for TB. Future Med. Chem 2011, 3, 1373–1400. [PubMed: 21879843]
7. Birch AJ; Holzapfel CW; Richards RW Diterpenoid Nature of Pleuromutilin. Chem. Ind 1963, 14, 374–375.
8. Stipkovits L; Ripley P; Tenk M; Glávits R; Molnár T; Fodor L The Efficacy of Valnemulin (Econor) in the Control of Disease Caused by Experimental Infection of Calves with Mycoplasma bovis. Res. Vet. Sci 2005, 78, 207–215. [PubMed: 15766939]

9. Jones RN; Fritsche TR; Sader HS; Ross JE Activity of Retapamulin (SB-275833), a Novel Pleuromutilin, against Selected Resistant Gram-Positive Cocci. Antimicrob. Agents Chemother. 2006, 50, 2583–2586. [PubMed: 16801451]
10. Novak R; Shlaes DM The Pleuromutilin Antibiotics: a New Class for Human Use. Curr. Opin. Invest. Drugs 2010, 11, 182–911.
11. Sader HS; Biedenbach DJ; Paukner S; Ivezic-Schoenfeld Z; Jonesa RN Antimicrobial Activity of the Investigational Pleuromutilin compound BC-3781 Tested against Gram-Positive Organisms Commonly Associated with Acute Bacterial Skin and Skin structure Infections. Antimicrob. Agents Chemother 2012, 56, 1619–1623. [PubMed: 22232289]
12. Paukner S; Sader HS; Ivezic-Schoenfeld Z; Jonesb RN Antimicrobial Activity of the Pleuromutilin Antibiotic BC-3781 against Bacterial Pathogens Isolated in the SENTRY Antimicrobial Surveillance Program in 2010. Antimicrob. Agents Chemother 2013, 57, 4489–4495. [PubMed: 23836172]
13. Hirokawa Y; Kinoshita H; Tanaka T; Nakata K; Kitadai N; Fujimoto K; Kashimoto S; Kojima T; Kato S Water-Soluble Pleuromutilin Derivative with Excellent In Vitro and In Vivo Antibacterial Activity against Gram-Positive Pathogens. J. Med. Chem 2008, 51, 1991–1994. [PubMed: 18330977]
14. Shang R; Wang G; Xu X; Liu S; Zhang C; Yi Y; Liang J; Liu Y Synthesis and Biological Evaluation of New Pleuromutilin Derivatives as Antibacterial Agents. Molecules 2014, 19, 19050–19065. [PubMed: 25415471]
15. Wang X; Ling Y; Wang H; Yu J; Tang J; Zheng H; Zhao X; Wang D; Chen G; Qui W; Tao J Novel Pleuromutilin Derivatives as Antibacterial Agents: Synthesis, Biological Evaluation and Molecular Docking Studies. Bioorg. Med. Chem. Lett 2012, 22, 6166–6172. [PubMed: 22932314]
16. Shang R; Pu X; Xu X; Xin Z; Zhang C; Guo W; Liu Y; Liang J Synthesis and Biological Activities of Novel Pleuromutilin Derivatives with a Substituted Thiadiazole Moiety as Potent Drug-Resistant Bacteria Inhibitors. J. Med. Chem 2014, 57, 5664–5678. [PubMed: 24892980]
17. Shang R; Wang S; Xu X; Yi Y; Guo W; Liu Y; Liang J Chemical Synthesis and Biological Activities of Novel Pleuromutilin Derivatives with Substituted Amino Moiety. PLoS One 2013, 8, e82595. [PubMed: 24376551]
18. Xu P; Z. Y. Y; Sun YX; Liu JH; Yang B; Wang YZ; Wang YL Novel Pleuromutilin Derivatives with Excellent Antibacterial Activity against *Staphylococcus aureus*. Chem. Biol. Drug Des 2009, 73, 655–660. [PubMed: 19635057]
19. Zhang YY; Xu KP; Ren D; Ge SR; Wang YL; Wang YZ Synthesis and Antibacterial Activities of Pleuromutilin Derivatives. Chin. Chem. Lett 2009, 20, 29–31.
20. Ling CY; Tao YL; Chu WJ; Wang H; Wang HD; Yang YS Design, Synthesis and Antibacterial Activity of Novel Pleuromutilin Derivatives with 4*H*-Pyran-4-one and Pyridin-4-one Substitution in the C-14 Side Chain. Chin. Chem. Lett 2016, 27, 235–240.
21. Tang YZ; Liu YH; Chen JX Pleuromutilin and Its Derivatives-the Lead Compounds for Novel Antibiotics. Mini-Rev. Med. Chem 2012, 12, 53–61. [PubMed: 22070694]
22. Long KS; Poehlsgaard LS; Hanse LH; Hobbie SN; Böttger EC; Vester B Single 23S rRNA Mutations at the Ribosomal Peptidyl Transferase Centre Confer Resistance to Valnemulin and Other Antibiotics in *Mycobacterium smegmatis* by Perturbation of the Drug Binding Pocket. Molecular Microbiology 2009, 71, 1218–1222. [PubMed: 19154331]
23. Lotesta SD, Liu J, Yates EV, Krieger I, Sacchettini JC, Freundlich JS, and Sorensen EJ Expanding the Pleuromutilin Class of Antibiotics by De Novo Chemical Synthesis. Chem. Sci, 2011, 2, 1258–1261. [PubMed: 21874155]
24. Dong YJ; Meng ZH; Mi YQ; Zhang C; Cui ZH; Wang P; Xu ZB Synthesis of Novel Pleuromutilin Derivatives. Part 1: Preliminary Studies of Antituberculosis Activity. Bioorg. Med. Chem. Lett 2015, 25, 1799–1803. [PubMed: 25736994]
25. Helmut E; Hellmuth R Substituted 14-Desoxy-Mutilin Compositions. U.S. Patent 4 278 674, 1981.
26. Knauseder F; Brandl E Ester Derivatives of Pleuromutilin. U.S. Patent 3 716 579, 1970.
27. Ramakrishnan Nagarajan. Pleuromutilin Glycoside Derivatives. U.S. Patent 4 130 709, 1977.
28. Biochemie GMBH, applicant. Mutilin Derivatives. GB Patent 1 312 148, 1973.

29. Ascher G; Berner H; Hildebrandt J Mutilin Derivatives and Their Use as Antibacterials. W.O. Patent 109 095, 2001.
30. Siricilla S; Mitachi K; Yang J; Eslamimehr S; Lemieux MR; Meibohm B; Ji Y; Kurosu M A New Combination of a Pleuromutilin Derivative and Doxycycline for Treatment of MDR *Acinetobacter baumannii*. J. Med. Chem. 2017, 60, 2869–2878. [PubMed: 28291943]
31. Wang Q; Wang Y; Kurosu M A New Oxyma Derivative for Nonracemizable Amide-forming Reactions in Wwater. Org. Lett. 2012, 14, 3372–3375. [PubMed: 22697488]
32. Wang Y; Aleiwi BA; Wang Q; Kurosu M Selective Esterifications of Primary Alcohols in a Water-containing Solvent. Org. Lett. 2012, 14, 4910–4913. [PubMed: 22937741]
33. Cho SH; Warit S; Wan B; Hwang CH; Pauli GF; Franzblau SG, Low-oxygen-recovery assay for high-throughput screening of compounds against nonreplicating *Mycobacterium tuberculosis*. Antimicrob Agents Chemother. 2007, 51, 1380–1385. [PubMed: 17210775]
34. Senthilraja P; Kathiresan. K In Vitro Cytotoxicity MTT Assay in Vero, HepG2 and MCF −7 Cell Lines Study of Marine Yeast J. Appl. Pharm. Sci 2015, 5, 80–84.
35. Kong Y; Yao H; Ren H; Subbian S; Cirillo SL; Sacchettini JC; Rao J; Cirillo JD, Imaging tuberculosis with endogenous β-lactamase reporter enzyme fluorescence in live mice. Proc Natl Acad Sci U S A 2010, 107, 12239–12244 [PubMed: 20566877]
36. Artursson P; Karlsson J Correlation between Oral Drug Absorption in Humans and Apparent Drug Permeability Coefficients in Human Intestinal Epithelial (Caco-2) Cells. Biochem. Biophys. Res. Comm. 1991, 175, 880–885. [PubMed: 1673839]
37. Falzari K; Zhu Z; Pan D; Liu H; Hongmanee P; Franzblau SG In Vitro and In Vivo Activities of Macrolide Derivatives against *Mycobacterium tuberculosis*. Antimicrob. Agents Chemother. 2005, 49, 1447–1454. [PubMed: 15793125]
38. Collins L; Franzblau SG Microplate alamar blue assay versus BACTEC 460 system for high-throughput screening of compounds against *Mycobacterium tuberculosis* and *Mycobacterium avium*. Antimicrob Agents Chemother 1997, 41, 1004–1009. [PubMed: 9145860]
39. Snewin VA; Gares MP; Gaora PO; Hasan Z; Brown IN; Young DB, Assessment of immunity to mycobacterial infection with luciferase reporter constructs. Infect. Immun 1999, 67, 4586–9453. [PubMed: 10456904]
40. Wang Z; Hop CE; Leung KH; Pang J Determination of *in vitro* permeability of drug candidates through a caco-2 cell monolayer by liquid chromatography/tandem mass spectrometry. J. Mass. Spectrom. 2000, 35, 71–76. [PubMed: 10633236]
41. Mitachi K; Yun H-G.; Kurosu SM; Eslamimehr S; Lemieux MR; Klaić L; Clemons WM, Jr.; Kurosu M Novel FR-900493 Analogs that Inhibit Outgrowth of Clostridium difficile Spores. ACS Omega 2018, 3, 1726–1739. [PubMed: 29503973]

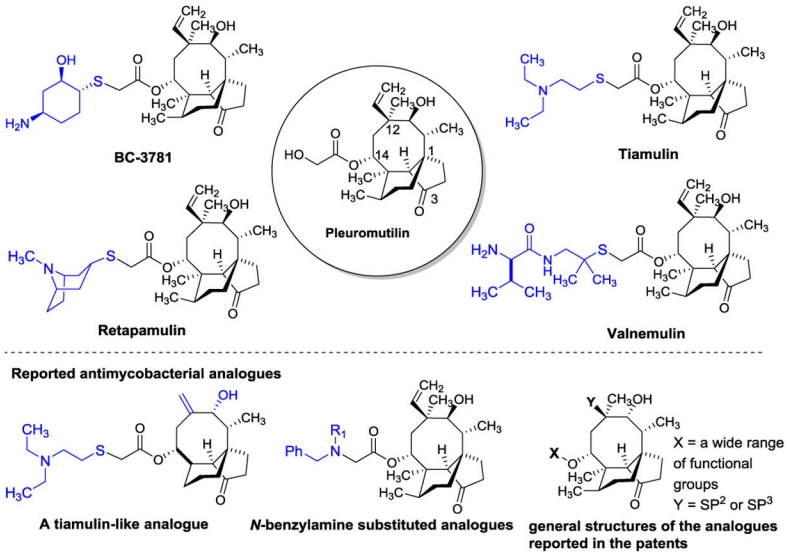

Figure 1.
Pleuromutilin and representative structures of pleuromutilin analogues.

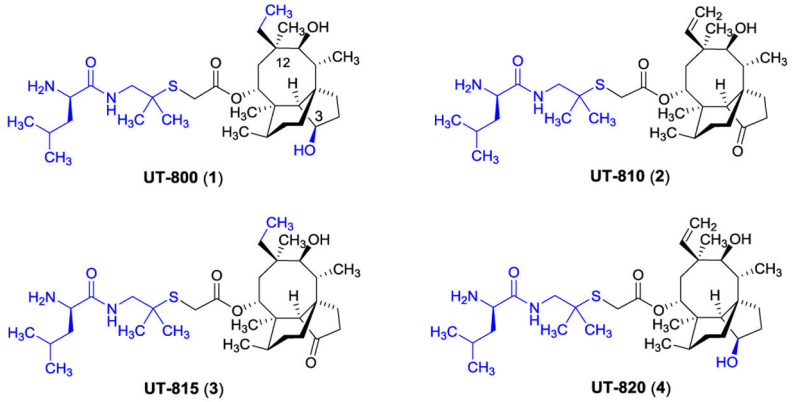

Figure 2.
Antimycobacterial Pleuromutilin analogues identified from our liabrary molecules.

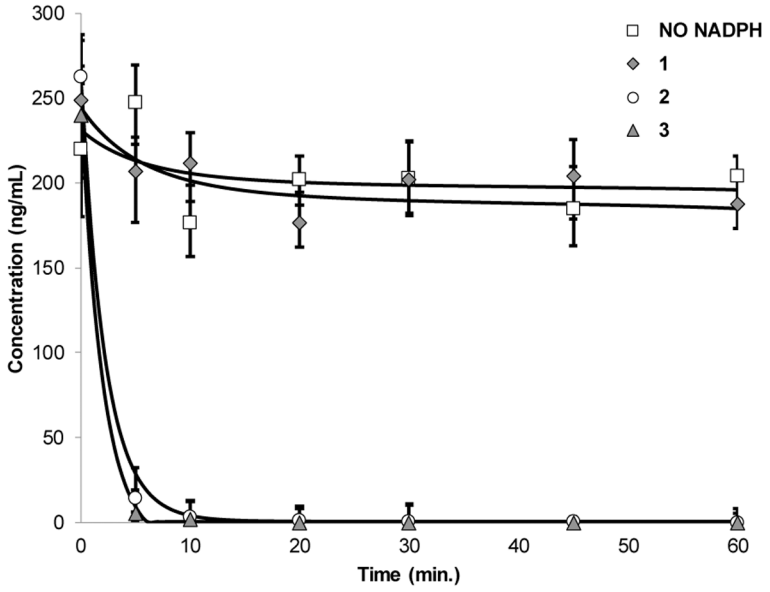

Figure 3.

Half life ($t_{1/2}$) of **1**–**3** in the rat liver microsomes[a]

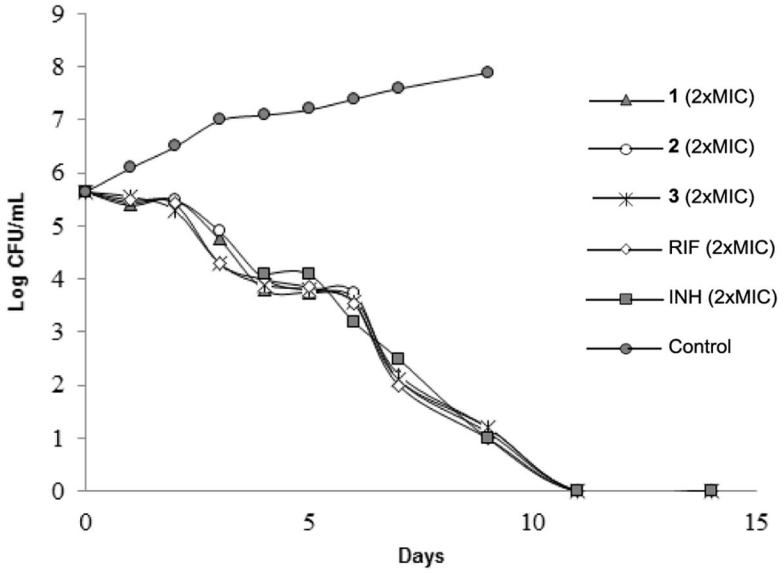

Figure 4.

In vitro time-kill assessment of **1**, **2** and **3** and the first-line TB drugs (RIF and INH).

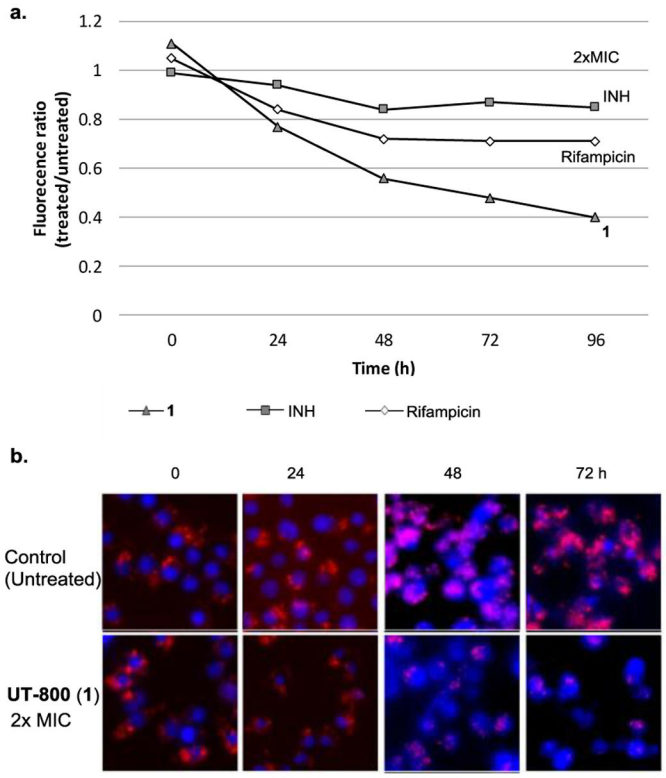

Figure 5.

Activity of **1** against non-replicating and intracellular Mtb CDC1551-tdTomato.

Mtb CDC1551-tdTomato a transforment Mtb CDC1551 containing tdTomato

a: Effect of **1**, INH and rifampicin (RIF) against intracellular Mtb CDC1551-tdTomato in macrophages (J774A.1 cells). Time-kill curve for intracellular Mtb at MIC x2 concentration.

b: Fluorescence confocal microscopy of J774A.1 murine macrophages infected with tdtomato (red) expressing Mtb after the treatment of the molecules at MICx2.

All images were obtained for the treated and untreated for 72h. Fixed cells were stained with a blue fluroscent stain, DAPI (4',6-diamidino-2-phenylindole) to visualize nuclei.

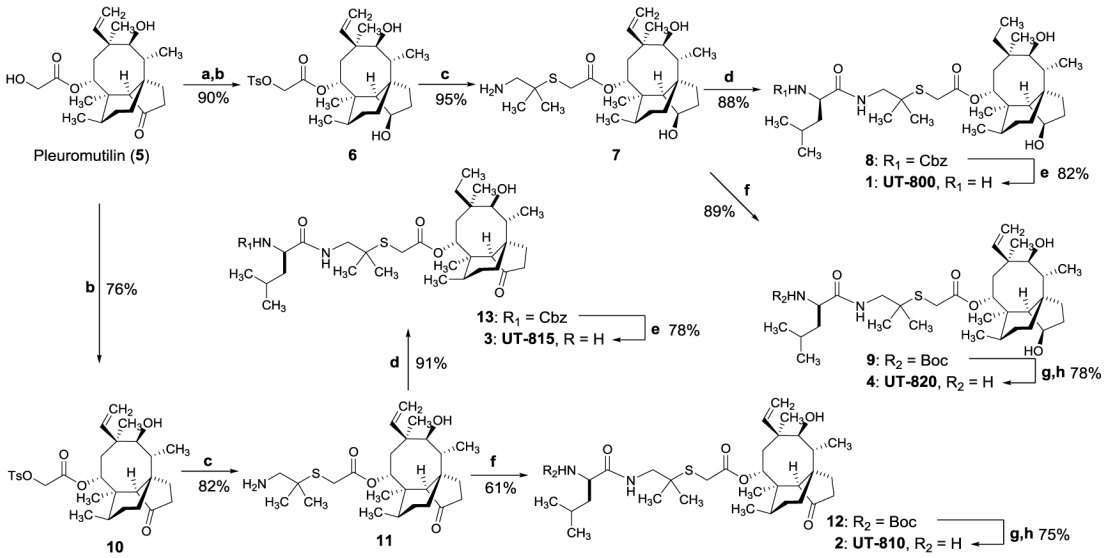

Conditions: **a**) $NaBH_4$, MeOH, 0 °C. **b**) TsCl, DMAP, CH_2Cl_2, 0 °C. **c**) 1-amino-2-methylpropane-2-thiol, 1M NaOH, $^nBu_4NBr$, THF/H_2O (1 : 1), 50 °C. **d**) Cbz-D-Leu-OH, Glyceroacetonide-Oxyma, EDCI, $NaHCO_3$, DMF-H_2O (9/1), **e**) H_2 / 10% Pd-C, MeOH-EtOAc (1/1). **f**) Boc-D-Leu-OH, Glyceroacetonide-Oxyma, EDCI, $NaHCO_3$, DMF-H_2O (9/1), **g**) 4*N* HCl (Dioxane). **h**) $NaHCO_3$ in MeOH.

Scheme 1.

Syntyheses of antimycobacterial pleuromutilin analogues **1**–**4**.

Table 1.

Transcription/Translation inhibition, MICs (Mtb) under aerobic and anaerobic conditions, and cytotoxicity (IC_{50}) of **1**-**4** and representative antibacterial agents.

Molecule	Transcription/ Translation inhibition at 0.1 μg/mL[a]	MIC μg/mL (MABA)[b]	MIC μg/mL (LORA)[c]	MIC_{LORA}/MIC_{MABA}	IC_{50} μg/mL Vero cells[d]	Selectivity Index (SI)[e]
UT-800 (1)	+++	0.83	1.20	1.45	25.0	**30.1**
UT-810 (2)	+++	1.56	1.98	1.27	25.0	**16.0**
UT-815 (3)	+++	0.78	1.04	1.33	25.0	**32.0**
UT-820 (4)	+++	3.06	3.46	1.13	35.0	**11.4**
Valnemulin	+++	3.13	3.56	1.14	15.0	**4.79**
Rifampicin (RIF)	ND	0.20	1.47	7.35	>200	**>1,000**
Isoniazid (INH)	ND	0.04–0.10	>100	>2,500	>200	**>2,000**
Ethambutol (EMB)	ND	0.78	>100	>128	>200	**>256**
Linezolid	+++	0.60	0.63	1.05	**>200**	**>333**

[a] The translation assay was performed with the Promega assay kit (L1020);

[b] MABA: microplate alamar blue assay;

[c] LORA: low-oxygen recovery assay;

[d] Cytotoxicity against Vero monkey kidney cells;

[e] Selectivity Index (SI) = IC_{50} (Vero cells)/MIC_{MABA}

Table 2.

Membrane permeability of **1** determined by Caco-2 assays.

Molecule	Test Conc. (μM)	Assay duration (h)	Mean A → B *P*app 10^{-6} cm/s^{-1}	Mean B → A *P*app 10^{-6} cm/s^{-1}	Efflux Ratio
Ranitidine	10.0	2.0	0.237	1.14	5.00
Talinolol	10.0	2.0	0.0517	3.92	76.8
UT-800(1)	10.0	2.0	3.39	18.3	5.44
Warfarin	10.0	2.0	35.2	28.0	0.794

Table 3.

Pharmacokinetic data for UT-800 (**1**).

a: IV administration (3 mg/kg)[1]

	$t_{1/2}$ (h)	C_{max} (ng/mL)	$AUC_{0\text{-}24h}$ (ng•h/mL)	AUC_{Inf} (ng•h/mL)
Mean	9.98	1,908	993	1,046

b: PO administration (30 mg/kg)[2]

	$t_{1/2}$ (h)	t_{max} (h)	C_{max} (ng/mL)	$AUC_{0\text{-}24h}$ (ng•h/mL)	AUC_{Inf} (ng•h/mL)	*F* (%)
Mean	4.02	0.83	1,344	2,869	2,891	27.6

c: PK parameters of 1 in serum and lung tissues (10 mg/kg IV)

Sample	$t_{1/2}$ (h)	C_{max} (ng/mL)	$AUC_{0\text{-}24h}$ (ng•h/unit)[3]
Serum	10.5	2,956	2,497
Lung	ND	6,074	66,281

[1] data were obtained using three BALB/c mice.

[2] data were obtained using six BALB/c mice. $t_{½}$: half-life; C_{max}: maximum concentration; t_{max}: time to maximum concentration (range); AUC: area under the concentration curve.

[3] Unit: mL for serum and g for lung.

Table 4.

Therapeutic efficacy of **1** against Mtb Erdman strain in a murine model via oral administration.

Molecule	Dosages (mg/kg)	Log_{10} cfu/mouse[1]	SD	Log reduction
Vehicle (water)	200	1.3E+06	3.8E+05	-
INH	2.5	7.8E+01	1.2E+02	4.22
UT-800 (1)	50	1.2E+06	2.6E+05	0.03
UT-800 (1)	100	8.1E+05	3.3E+05	0.20
UT-800 (1)	200	4.4E+05	2.4E+05	0.47

[1] Each value represents the mean ± SD for 5 mice.